Materials Letters 181 (2016) 331–334

Contents lists available at ScienceDirect

Materials Letters

journal homepage: www.elsevier.com/locate/matlet

# Influence of particle size on the adsorption and release of cephalexin encapsulated in mesoporous silica SBA-15

María Soledad Legnoverde [a,b], Elena I. Basaldella [a,*]

[a] Centro de Investigación y Desarrollo en Ciencias Aplicadas (CINDECA), Facultad de Ciencias Exactas, Universidad Nacional de La Plata – CONICET, Calle 47 N ° 257, B1900AJK La Plata, Argentina

[b] Centro de Investigación y Desarrollo en Ciencia y Tecnología de Materiales (CITEMA), Universidad Tecnológica Nacional, Facultad Regional la Plata, Calle 60 y 124, B1923 Berisso, Argentina

ARTICLE INFO

*Article history:*
Received 27 October 2015
Received in revised form
2 May 2016
Accepted 11 June 2016
Available online 13 June 2016

*Keywords:*
Sba-15
Particle size
Adsorption
Drug delivery
Cephalexin

ABSTRACT

Ordered mesoporous silicas with different particle sizes were synthesized and used as drug carrier in controlled delivery systems. Morphological properties of mesoporous supports were modified by changing the stirring rate. Changes in the shape of SBA-15 from fiber-like particles to smaller irregular agglomerates were obtained by reducing the stirring rate. The adsorption and release of cephalexin from those different supports were investigated. Adsorption capacity was found to increase with decreasing particle sizes, and the *in vitro* release experiments indicated a clear increase in the amount released from the smaller particles. *In vivo* studies revealed that silica matrixes effectively control the drug release and were capable of maintaining a sustained therapeutic blood level of cephalexin.



## 1. Introduction

Ordered mesoporous silicas have unique characteristics such as uniform pore size, high surface area, high mechanical strength and good thermal stability at wide temperature ranges. These properties provide great versatility to those materials for different technological applications, particularly in mass transfer processes such as adsorption and immobilization of substances [1–4].

The use of nanotechnology in medicine and more specifically in drug delivery systems is set to spread rapidly. Several drug delivery systems recently studied propose the use of mesoporous silicas as drug carriers [5–9]. Such studies were intended to prove that these porous materials are capable of releasing a carried bioactive agent at a specific rate. The main aim of these new systems is to facilitate the dosage and duration of the drug effect, in order to cause minimal disturbance to the patient by allowing the reduction of the dosage frequency. The particle size and morphology, as well as the size, volume and geometry of the pores, are all important parameters determining the release rate of the incorporated drug molecules [10–14]. An interesting review about the different types and bioapplications of mesoporous materials indicates that mesostructured silicas can nowadays be considered as one of the most efficient matrices for drug delivery [15].

Long-acting release formulations for subcutaneous administration would be a good therapeutic option when oral administration is restricted (vomiting) or difficult (for fractious animals). In previous work we demonstrated that cephalexin could successfully be loaded on SBA-15 mesoporous silica [16–18]. Cephalexin is a semisynthetic first-generation cephalosporin, with great gram-positive coverage and some activity against gram-negative bacteria, which is indicated for the treatment of various infections, including bone, joint and dental infections [19]. Additionally, the biocompatibility of SBA-15 was analyzed. Previous biopsy results obtained after injection of physiological solution containing SBA-15 particles to a group of rats sacrificed in a $CO_2$ chamber showed that irritation or inflammation was not detected in the skin [20]. To go further in this research, in this work we evaluate the *in vitro* adsorption and drug release of cephalexin from SBA-15 silicas possessing different particle sizes. Results for *in vivo* release were also obtained.

## 2. Experimental

SBA-15 materials were synthesized according to the procedure reported by Zhao et al. [21] by using tetraethylorthosilicate (TEOS; Aldrich) as silica source and Pluronic 123 triblock copolymer (P123, EO20-PO70-EO20; Aldrich) as template. The molar composition used was 1TEOS:4.88HCl:0.0172Pluronic:158 · 33$H_2O$. The

* Corresponding author at: Centro de Investigación y Desarrollo en Ciencias Aplicadas (CINDECA), Facultad de Ciencias Exactas, Universidad Nacional de La Plata – CONICET, Calle 47 N° 257, B1900AJK La Plata, Argentina.
*E-mail address:* eib@quimica.unlp.edu.ar (E.I. Basaldella).

http://dx.doi.org/10.1016/j.matlet.2016.06.053
0167-577X/

solution was heated up to 35 °C before adding the TEOS. The resulting solution was stirred for 20 h at 35 °C, followed by aging at 80 °C for 24 h under static conditions. The solid product was recovered by filtration and dried at room temperature overnight. The template was removed from the as-made mesoporous material by calcination at 540 °C for 6 h. Different size particles were obtained by modification of the stirring rate (120 and 400 rpm) [22]. The samples were called $SBA_{120}$ and $SBA_{400}$.

SEM micrographs were obtained by using a Scanning Electron Microscope Philips 505. Transmission electron microscopy (TEM) was performed with a Leo EM-910 instrument operated at 120 kV. The adsorption-desorption nitrogen isotherms were measured at −196 °C using Micromeritics apparatus ASAP 2020 (Micromeritics, Atlanta, Georgia). The Brunauer–Emmett–Teller (BET) equation was used to calculate the surface area in the range of relative pressures between 0.05 and 0.20. The pore size distribution was obtained by the BJH method, using the adsorption branch of the loop. The pore volume was taken at the $P/P_0=0.989$ single point.

The two SBA-15 samples were soaked in a solution of cephalexin (CPX) in water (concentration 1 mg/mL). The resulting suspensions (1 mg solid/mL liquid) were left at ambient temperature, with stirring for 6 h. The solid phases were separated from the liquids by filtration and dried at room temperature. The respective samples were denoted as $SBA_{120}$/cpx and $SBA_{400}$/cpx.

For drug release experiments, 0.2 g. of prepared samples ($SBA_{120}$/cpx and $SBA_{400}$/cpx) were put in contact with 1000 mL of simulated body fluid (SBF) [23]. The cephalexin content in the liquid phase was determined by UV–visible spectroscopy at 262 nm (UV-1800 Shimadzu, Japan).

The *in vivo* study was carried out in three healthy New Zealand white rabbits 3.0–3.5 kg in weight. All animal procedures were approved by the Institutional Animal Care and Use Committee, School of Veterinary, University of La Plata, Argentina. Animals received the 10% w/v of $SBA_{400}$/cpx formulation at a dose rate of 60 mg/kg by subcutaneous (SC) injection. Blood samples (0.4 mL) were collected in K-EDTA, through a 24 G x ¾" intravenous catheter (Introcan®, Braun Aß, Germany) placed in the marginal ear vein, at 0.5, 0.75, 1, 6, 12, 24, 48, 72 and 96 h post-administration. Cephalexin plasma concentration was determined by microbiological assay [24]. The limit of detection and quantification of the method were 0.19 and 0.39 μg/mL, respectively. Inter and intra-assay coefficients of variation were 9.39% and 4.87%, respectively.

## 3. Results and discussion

Fig. 1 shows SEM micrographs of the solids obtained. It can be seen that a high stirring rate (400 rpm) leads to particles with the same size and shape (fiber-like) as conventional SBA-15 reported by Zhao et al. [21]. A decrease in the stirring rate to 120 rpm produces a significant decrease in particle size. According to Zhao et al. [25], highly energetic organic–inorganic interfaces favor fiber formation, whereas systems with low energy lead to morphologies with lower energy and smaller in size. Fig. 2 displays the $N_2$ sorption isotherms recorded for the obtained silicas. Type IV adsorption isotherms with an H1 hysteresis loop (according to the IUPAC classification) were observed [26]. For the two samples, typical capillary condensation was observed within a relative pressure range of 0.4–0.8, reflecting the presence of mesopores. This result is in good agreement with the related TEM analysis (Fig. S1). The sharpness of the two loops indicates that both silicas have narrow pore size distributions. The partial pressure related to the onset of hysteresis indicates an averaged mesopore diameter that is smaller for $SBA_{120}$ (3.5 nm) than for $SBA_{400}$ (4.5 nm). Table S.1 summarizes the textural properties of SBA-15 materials prepared with different stirring rates.

The adsorption kinetic curves showed that the equilibrium time for $SBA_{120}$ and $SBA_{400}$ was 5.5 h and 5 h, respectively (Fig. 3. A). $SBA_{120}$ shows higher adsorption capacity of CPX than $SBA_{400}$. This may be attributed to the difference in their particle sizes. Smaller particles increase the probability of access of the CPX molecule to pores of the siliceous matrix. The conventional material presenting larger particle size leads to slower adsorption due not only to the possibility of pore blockage by the cephalexin molecules entering through the silica pore channels, but also to their increased pore length and tortuosity. Therefore, it is unlikely that complete monolayer coverage of the internal surface area could be achieved. Additionally, it has to be noted that $SBA_{120}$ presents a smaller pore diameter than $SBA_{400}$ (Table S.1), but the cephalexin size (about 1 nm) is by far smaller than the $SBA_{120}$ pore size.

*In vitro* CPX release profiles of all drug-loaded materials were linear at the initial drug release stage on the plot. The particle size of the materials affects the adsorption capacity, and also alters the amount of drug released. The $SBA_{400}$ support releases a lower amount of cephalexin than the $SBA_{120}$ according to the particle size and the decreased tortuosity in diffusional path (Fig. 3. B). The initial drug release from SBA-15 was very rapid, but the release slowed down considerably after 10 h. The total drug released from $SBA_{120}$ and $SBA_{400}$ was about 85% and 60%, respectively. Adverse

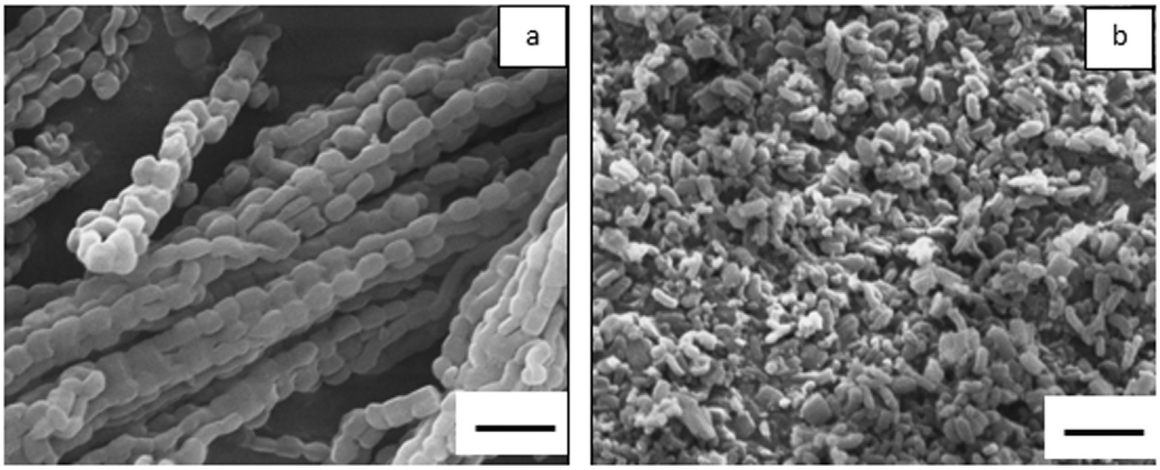


**Fig. 1.** SEM images of SBA-15 materials obtained at different stirring rates. a) $SBA_{400,}$ bar $=2$ μm; b) $SBA_{120}$, bar$=2$ μm.

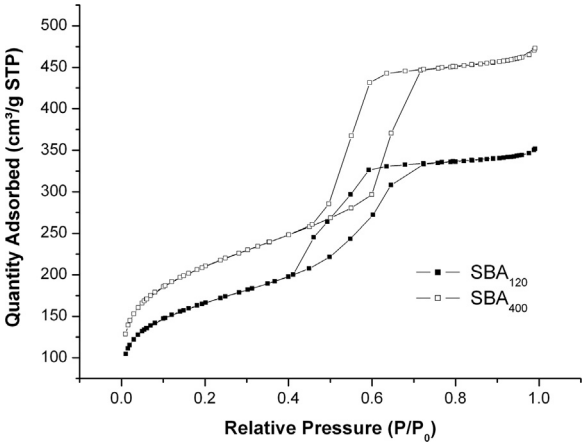


**Fig. 2.** $N_2$ adsorption/ desorption isotherms for $SBA_{120}$ and $SBA_{400}$.

effects usually associated to subcutaneous injection (skin irritation or inflammation) were not observed during or following CPX administration in any of the experimental animals. CPX mean plasma concentration *versus* time curves obtained after SC administration are shown in Fig. 3. C. The plot shows two peak concentrations, where the first peak observed at short times indicates the burst release of the drug [27]. A second high concentration peak is observed at 72 h, probably caused by a partial degradation of the silica particles, increasing the drug release [28]. Therefore, nanoencapsulation of CPX resulted in a controlled drug release, and it rendered a sustained drug concentration in plasma for about 90 h.

## 4. Conclusions

The influence of SBA-15 particle size on cephalexin adsorption and further release was studied. A diminution in the particle size produces an increase in the adsorption capacity, and also alters the amount of drug released. According to its smaller particle size and decreased tortuosity for diffusional path, $SBA_{120}$ releases a higher amount of cephalexin compared to $SBA_{400}$. In addition, *in vivo* pharmacokinetic analysis of $SBA_{400}$/cpx in rabbits showed a sustained release of cephalexin for more than 72 h. Our studies show for the first time the presence of a sustained cephalexin level in the blood achieved by injecting a drug-impregnated SBA-15.

## Acknowledgments

The authors thank Dr F. Landoni and Dr M. L. Meneses from the Facultad de Ciencias Veterinarias, La Plata National University, for their help in conducting the *in vivo* experiments. The authors would like to thank CIC and UTN (Grant No. I25062) for financial support. E. I. Basaldella is member of CIC-PBA.

## Appendix A. Supplementary material

Supplementary data associated with this article can be found in the online version at http://dx.doi.org/10.1016/j.matlet.2016.06.053.

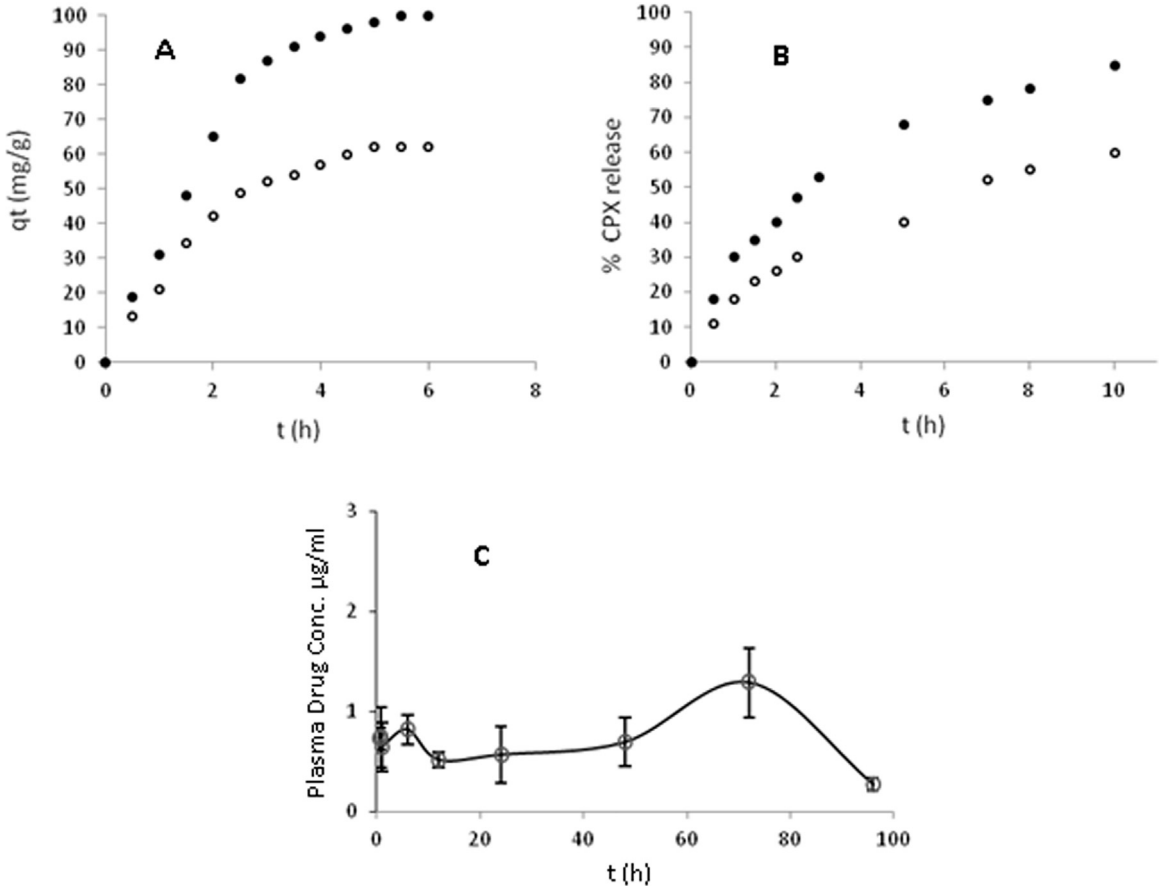


**Fig. 3.** A) Adsorption kinetics of CPX, B) Release kinetics of CPX, C) Plasma concentration (µg/mL) of cephalexin at various time intervals after subcutaneous injection of $SBA_{400}$/cpx. (●) $SBA_{120}$ and (○) $SBA_{400}$.

## References


[1] T.X. Bui, H. Choi, Adsorptive removal of selected pharmaceuticals by mesoporous silica SBA-15, J. Hazard Mater. 168 (2009) 602–608.

[2] Ch.H. Lee, T.S. Lin, Ch.Y. Mou, mesoporous materials for encapsulating enzymes, Nano Today 4 (2009) 165–179.

[3] G. Li, Z. Zhao, J. Liu, G. Jiang, Effective heavy metal removal from aqueous systems by thiol functionalized magnetic mesoporous silica, J. Hazard Mater. 192 (2011) 277–283.

[4] L.S. Mendes, S. Saska, M.A.U. Martines, R. Marchetto, Nanostructured Materials based on *meso*porous Silica and *meso*porous Silica/Apatite as osteogenic Growth Peptide Carriers, Mat. Sci. Eng. C 33 (2013) 4427–4434.

[5] T. López, E.I. Basaldella, M.L. Ojeda, J. Manjarrez, R. Alexander-Katz, Encapsulation of valproic acid and sodic phenytoin in ordered mesoporous $SiO_2$ solid for the treatment of temporal lobe epilepsy, Opt. Mater. 29 (2006) 75–81.

[6] Ch.X. Lin, S.Z. Qiao, Ch.Z. Yu, S. Ismadji, G.Q. Lu, Periodic *meso*porous Silica and organosilica with Controlled morphologies as cARrIERS FOR DRUG RELEASE, Micro. Mesopor Mater 117 (2009) 213–219.

[7] A. Szegedi, M. Popova, I. Goshev, J. Mihály, Effect of amine functionalization of spherical MCM-41 and SBA-15 on controlled drug release, J. Solid State Chem. 184 (2011) 1201–1207.

[8] S.Y. Park, P. Pendleton, *meso*porous silica SBA-15 for natural antimicrobial delivery, Powder Technol. 223 (2012) 77–82.

[9] F. Sevimli, A. Yılmaz, Surface functionalization of SBA-15 particles for amoxicillin delivery, Micro. Mesopor Mater. 158 (2012) 281–291.

[10] H. Gustafsson, E.M. Johansson, A. Barrabino, M. Odén, K. Holmberg, Immobilization of lipase from *Mucor miehei* and *Rhizopus oryzae* into mesoporous silica The effect of varied size and morphology, Colloids Surf. B Biointerfaces 100 (2012) 22–30.

[11] Y. Ding, G. Yin, X. Liao, Z. Huang, X. Chen, Y. Yao, J. Li, A convenient route to synthesize SBA-15 rods with tunable pore length for lysozyme adsorption, Micro. *meso*por Mater. 170 (2013) 45–51.

[12] H. Wang, P. Van Der Voort, H. Qu, S. Liu, A simple room-temperature synthesis of mesoporous silica rods with tunable size and porosity, J. Nanopart. Res. 15 (2013) 1501.

[13] L. Li, Y. Sun, B. Cao, H. Song, Q. Xiao, W. Yi, Preparation and performance of polyurethane /mesoporous silica composites for coated urea, Mater. Des. (2016), http://dx.doi.org/10.1016/j.matdes.2016.03.043.

[14] M. Geszke-Moritz, M. Moritz, APTES-modified mesoporous silicas as the carriers for poorly water-soluble drug. Modeling of diflunisal adsorption and release, Appl. Surf. Sci. 368 (2016) 348–359.

[15] M. Moritz, M. Geszke-Moritz, *meso*porous materials as multifunctional tools in biosciences: Principles and applications, Mater. Sci. Eng C. 49 (2015) 114–151.

[16] E.I. Basaldella, M.S. Legnoverde, Functionalized silica matrices for controlled delivery of cephalexin, J. Sol.-Gel Sci. Technol. 56 (2010) 191–196.

[17] D.P. Vargas, M.S. Legnoverde, L. Giraldo, E.I. Basaldella, J.C. Moreno, Preparation and characterization of textural and energetic parameters of common and functionalized SBA-15 mesoporous silica, Adsorpt. Sci. Technol. 28 (2010) 387–396.

[18] M.S. Legnoverde, I. Jiménez-Morales, E. Rodríguez-Castellón, A. Jiménez-Morales, E.I. Basaldella, Modified alexin, Med Chem. 9 (2013) 672–680.

[19] T.J. Franklin, G.A. Snow, Biochemistry of Antimicrobial Action, Chapman & Hall., London 1981, pp. 45–46.

[20] T. López, E. Krötzsch, E. Ortiz-Islas, M. Alvarez-Lemus, E. Balsadella, J. M. Martínez-Blanes, J.A. Odriozola, Release properties and acute biosecurity determination of collagen-polyvinylpyrrolidone loaded in ordered mesoporous silica, Key Eng. Mater. 391 (2009) 169–184.

[21] D. Zhao, Q. Huo, J. Feng, B.F. Chmelka, G.D. Stucky, Triblock Copolymer Syntheses of *meso*porous Silica with Periodic 50–300 Angstrom Pores, Sci 279 (1998) 548–552.

[22] A. Carrero, J. Moreno, J. Aguado, G. Calleja, Control of SBA-15 materials morphology by modification of synthesis conditions, Stud. Surf. Sci. Catal. 174 (2008) 321–324.

[23] T. Kokubo, H. Kushitani, S. Sakka, T. Kitsugi, T. Yamamuro, Solutions able to reproduce in vivo surface-structure changes in bioactive glass-ceramic A-W3, J. Biomed. Mater. Res. 24 (1990) 721–734.

[24] J.V. Bennet, J.L. Brodie, E.J. Bennet, W. Kirby, Simplified accurate method for antibiotic assay of clinical specimens, Appl. Microbiol. 14 (1966) 170–177.

[25] D. Zhao, J. Sun, Q. Li, G.D. Stucky, Morphological Control of Highly Ordered *meso*porous Silica SBA-15, Chem. Mater. 12 (2000) 275–279.

[26] S. Lowell, J.E. Shields, M.A. Thomas, M. Thommes, Characterization of Porous Solids and Powders: Surface Area, Pore Size and Density, Kluwer Academic Publishers, 2003.

[27] A. Hatefi, B. Amsden, Biodegradable injectable in situ forming drug delivery system, J. Control Release 80 (2002) 9–28.

[28] B.C. Anderson, N.K., Pandit N.K., S.K, Mallapragada. Understanding drug release from poly(ethylene oxid)e)( – 5b-poly(propylene oxid)e)(-b-poly(ethylene oxid)e) (gels). J Control Release, 2001, 70. pp. 157–167.